

# Binocular cross-correlation analyses of the effects of high-order aberrations on the stereoacuity of eyes with keratoconus

Sangeetha Metlapally

School of Optometry, UC Berkeley, Berkeley, CA, USA



Shrikant R. Bharadwaj

Brien Holden Institute of Optometry and Vision Sciences,  
LV Prasad Eye Institute, Telangana, India

Austin Roorda

School of Optometry, UC Berkeley, Berkeley, CA, USA

Vinay Kumar Nilagiri

Brien Holden Institute of Optometry and Vision Sciences,  
LV Prasad Eye Institute, Telangana, India

Tiffanie T. Yu

School of Optometry, UC Berkeley, Berkeley, CA, USA

Clifton M. Schor

School of Optometry, UC Berkeley, Berkeley, CA, USA

Stereoacuity losses are induced by increased magnitudes and interocular differences in high-order aberrations (HOAs). This study used keratoconus as a model to investigate the impact of HOAs on disparity processing and stereoacuity. HOAs and stereoacuity were quantified in subjects with keratoconus ( $n = 21$ ) with HOAs uncorrected (wearing spectacles) or minimized (wearing rigid gas-permeable contact lenses) and in control subjects without keratoconus ( $n = 5$ ) for 6-mm pupil diameters. Disparity signal quality was estimated using metrics derived from binocular cross-correlation functions of stereo pairs convolved with point-spread functions from these HOAs. Metrics computed for all subjects were compared with stereoacuties. The effects of contrast losses and phase shifts on disparity signal quality were studied independently by manipulating the amplitude and phase components of optical transfer functions. The magnitudes, orientations, interocular relationships in magnitude, and shape of the point-spread function affected the cross-correlation metrics that determine disparity signal quality. Stereoacuity covaries strongly with cross-correlation metrics and moderately with image-quality metrics. Both phase distortions and contrast losses due to HOAs significantly influence computations of binocular disparity. HOA-induced stereoacuity reductions are attributable to disparity blur and noise from image properties that reduce the height and kurtosis of the peak stimulus

disparity match of the cross-correlation. Phase distortions and contrast losses due to HOAs are both partly responsible for the greater stereoacuity losses seen with spectacles compared to rigid gas-permeable contact lenses in keratoconus.

## Introduction

Stereoscopic depth perception is one of the key advantages of binocular vision. It is achieved by calculating horizontal binocular retinal disparity along with estimates of azimuth and distance (Gillam, Chambers, & Lawergren, 1988; Howard & Rogers, 2012; Mayhew & Longuet-Higgins, 1982). Loss of depth perception is associated with deficits in performance of certain motor skills and leads to self-reported problems that lower the vision-related quality of life (Fielder & Moseley, 1996; Frost et al., 1998; O'Connor, Birch, Anderson, Draper, & FSOS Research Group, 2010). Stereoscopic depth perception relies upon high-quality retinal images of the two eyes that are then matched to each other, to obtain high-fidelity estimates of binocular disparity. Thus, stereoacuity is intimately related to optical quality, as determined by optical wavefront aberrations of the two eyes.

Citation: Metlapally, S., Bharadwaj, S. R., Roorda, A., Nilagiri, V. K., Yu, T. T., & Schor, C. M. (2019). Binocular cross-correlation analyses of the effects of high-order aberrations on the stereoacuity of eyes with keratoconus. *Journal of Vision*, 19(6):12, 1–20, <https://doi.org/10.1167/19.6.12>.

<https://doi.org/10.1167/19.6.12>

Received October 19, 2018; published June 11, 2019

ISSN 1534-7362 Copyright 2019 The Authors



Monochromatic wavefront aberrations of the eye may be classified into low-order aberrations (LOAs; i.e., defocus and astigmatism) that are correctable using sphero-cylindrical spectacles and high-order aberrations (HOAs) that are not correctable using sphero-cylindrical spectacles. Predictably, stereoacuity deteriorates with increasing magnitudes and interocular differences in optical blur due to LOAs (Hess, Liu, & Wang, 2003; Westheimer & McKee, 1980; Wood, 1983). This has been demonstrated with monocularly induced defocus blur by convex lenses (Levy & Glick, 1974; Lovasik & Szymkiw, 1985; Wood, 1983), astigmatic blur produced by cylindrical lenses (Chen, Hove, McCloskey, & Kaye, 2005), filtered images that are devoid of high-spatial-frequency information (Hess et al., 2003; Wood, 1983), and naturally occurring interocular differences in visual acuity (Lam, Chau, Lam, Leung, & Man, 1996).

The effects on stereoacuity of optical blur due to HOAs have received less attention, perhaps because of the low levels of HOAs seen in the general human population and the minor disturbance they cause to visual performance (Thibos, Hong, Bradley, & Cheng, 2002). Stereoacuity (i.e., the smallest disparity that stimulates stereo depth) and the upper disparity limit (i.e., the largest disparity that stimulates stereo depth) are correlated with the overall magnitude and interocular differences in HOAs. More specifically, stereoacuity is worse in subjects with keratoconus and with surgical interventions like penetrating keratoplasty for corneal transplantation and LASIK refractive surgery, where HOAs are increased and mismatched between eyes (Bandela, Satgunam, Garg, & Bharadwaj, 2016; Nilagiri, Metlapally, Kalaiselvan, Schor, & Bharadwaj, 2018). On the other hand, the upper disparity limit that goes beyond the limit of binocular fusion (Duwaer, 1983; Howard & Rogers, 2012) is lowered with increasing interocular differences of HOAs (Jimenez, Castro, Hita, & Anera, 2008). Also, stereoacuity losses are partially recovered when subjects switch from sphero-cylindrical spectacles to rigid gas-permeable contact lenses (RGP CLs) that minimize HOAs (Bandela et al., 2016; Nilagiri et al., 2018).

The optical blur produced by monochromatic aberrations affects image quality by producing both contrast losses and phase shifts in the retinal image, the magnitudes of which depend on the spatial-frequency content of the objects in the scene. Stereoacuity is determined by the monocular image quality and interocular relationships in image quality. It deteriorates with an overall reduction of contrast in both eyes and with increasing interocular differences in contrast (Castro, Jimenez, Hita, & Ortiz, 2009; Cormack, Stevenson, & Landers, 1997; Cormack, Stevenson, & Schor, 1991). However, the impact on stereoacuity of interocular differences in phase shifts is not readily

available. Understanding this relationship is arguably very important, especially for aberrations that are not rotationally symmetric (e.g., coma), which are seen in large magnitudes in keratoconus. Different phase distortions for the two eyes would conceivably introduce disparity noise, which could reduce the number of retinal pattern elements aligned with the stimulus disparity and adversely affect stereoacuity.

Three important questions related to the impact of optical quality of the retinal image on binocular disparity are addressed in this article. First, how are the binocular cross-correlation metrics influenced by HOAs, and what are the relationships, if any, between the computed metrics and empirically derived stereoacuity? Second, how are image-quality (IQ) metrics influenced by HOAs and how are they correlated with stereoacuity loss? Third, what are the independent contributions to the binocular cross-correlation function of phase distortions and contrast loss of the optical transfer function (OTF) due to HOAs?

We addressed these questions utilizing a cross-correlation model of the binocular matching process that describes the coding of binocular disparity (Banks, Gepshtein, & Landy, 2004; Cormack et al., 1991). Specifically the analyses shed light on how the magnitudes, shapes, centration, orientation, and interocular relationships of blur (the complex point-spread function [PSF]) influence computing depth from disparity. They demonstrate contributions to stereoacuity loss in keratoconus from both contrast loss and phase distortions due to HOAs. In addition, these computational analyses reveal relationships and relative contributions of the phase and contrast components of the OTF that would be difficult to demonstrate in empirical experiments (e.g., by phase correcting the OTF).

## General methods

### Empirical measures

Descriptive data on the subject population and the empirical data-collection protocols are described in detail by Nilagiri et al. (2018), and methods relevant to the current article are described in the following sections. Empirical measures of wavefront aberrations and stereoacuity were collected from a random subset of subjects with unilateral ( $n = 9$ ) and bilateral ( $n = 12$ ) keratoconus and control subjects ( $n = 5$ ) with best-corrected monocular high-contrast logMAR visual acuity of 20/20 or better with spectacles. All subjects with keratoconus were experienced RGP CL users of  $\geq 1$  year with no complaints with their current contact lenses and an average CL wear time of  $\geq 8$  hr/day.

Subjects who had any signs of corneal insult due to RGP CL wear, apical scarring, superficial punctate keratitis, conjunctival congestion, history of binocular eye deviations, frequent blink rate, intolerance to longer durations of lens wear, or best-corrected CL vision of  $<20/30$  were excluded from the study. All subjects signed a written informed-consent form approved by the institutional review board at the LV Prasad Eye Institute. All study procedures adhered to the tenets of the declaration of Helsinki.

### **Wavefront-aberration measurements**

High-order (third- to sixth-order Zernike) wavefront aberrations were measured postcycloplegia over 6-mm pupil diameter using an irx3 wavefront aberrometer (Imagine Eyes SA, Orsay, France; specification data-sheet available at <http://www.imagine-eyes.com/product/irx3/>). These were used to model the influence of contrast losses and phase distortions due to HOAs on disparity maps of cross-correlated random-dot (RD) stereograms. All subjects were measured unaided by optical correction. Data from control subjects are presented in the results as the Control conditions, and data from subjects with keratoconus measured in this manner are presented as the HOA uncorrected condition. Subjects with keratoconus were measured additionally through their habitual RGP CLs (HOA minimized condition) and were eliminated from the study if measurements were not possible due to CL movement on the eye or if the measurement ranges were beyond device specifications due to disease severity. Subjects were measured three times for each of the conditions (HOA uncorrected, HOA minimized, and Control). Zernike aberrations for pupils  $>6$  mm were scaled to pupil sizes of 6 mm before data were exported for further analyses.

### **Refraction and stereoacuity measurements**

Objective (retinoscopy) and subjective (trial-frame) postcycloplegic refractions were performed using standard clinical procedures by one investigator at the LV Prasad Eye Institute. Subjective refraction was performed through 6-mm apertures using letter targets on a COMPlog (Complog Clinical Vision Measurement Systems Ltd, London, UK; <http://complog-visual-acuity.com/>) monitor at a viewing distance of 3 m. A similar procedure was performed for overrefraction through RGP CLs in subjects with keratoconus, and logMAR visual acuities for all conditions were documented.

Stereoacuity was measured at a viewing distance of 40 cm with RD stereo images presented on an LCD monitor and controlled using custom Psychophysics Toolbox MATLAB software (MathWorks, Natick,

MA; Brainard, 1997; Pelli, 1997). Under active cycloplegia, subjects viewed stimuli through their best-corrected-distance refractive correction and 6-mm artificial apertures in a trial frame. Subjects held a Screen-VU stereo viewer device (PS Manufacturing, Portland, OR), which is a form of Brewster stereoscope with built-in near correction, to view and fuse two side-by-side RD stereo images. The RD stimuli in each presentation were two  $7^\circ \times 7^\circ$  square patches with 1,500 white dots on a black background (dot density = 45 dots/ $^\circ^2$ ), with a central fixation cross that allowed subjects to maintain stable binocular fixation throughout the experiment. The subjects' task was to identify the tilt orientation (right or left) of a rectangular bar seen in cyclopean depth within the RD patterns. Stereo stimuli were displayed for 1,000 ms, with an interval of 200 ms between successive stimuli. This exposure time is adequate to test for form identification of the RD stereogram, which involves more complex processing (Harwerth & Rawlings, 1977). Disparity amplitude of the rectangle was quantified from the viewing distance and viewing angle, which was converted from degrees to arc seconds. Subjects were acquainted with the staircase procedure via a short training session, both prior to and following cycloplegia. The set of three trials for subjects with keratoconus was performed first with spectacles and then repeated with RGP CLs. This sequence avoided any influence of potential short-term changes in the corneal surface caused by RGP CLs on estimates of stereoacuity. Stereo thresholds were not measured without optical corrections in keratoconus, because the thresholds were beyond the limits of the system.

## **Computational methods**

### **The cross-correlation model**

The cross-correlation analysis utilized aberration measurements, obtained from highly aberrated eyes of subjects with keratoconus, to estimate the effects of optical degradation of the retinal image on binocular disparity processing (Banks et al., 2004; Cormack et al., 1991; Doi, Tanabe, & Fujita, 2011; Filippini & Banks, 2009; Tyler, 1978). Analyses were performed using custom programs written in MATLAB. An RD image consisting of 1,800 black dots on a white background (dot density = 78 dots/ $^\circ^2$ ) and overall size of  $5^\circ \times 5^\circ$  square was used to form stereo pairs for computing the binocular cross correlation. The stereogram used to compute the cross correlation was a zero-disparity or flat RD stereogram with no depth variation from the frontoparallel plane. This RD pattern was used to emphasize the influence of optical degradation on the sharpness and amplitude of the peak of the cross-correlation function. For all conditions, LOAs were set to 0  $\mu\text{m}$  and PSFs of right and left eyes were derived only from HOAs for 6-mm pupils. Nulling the Zernike

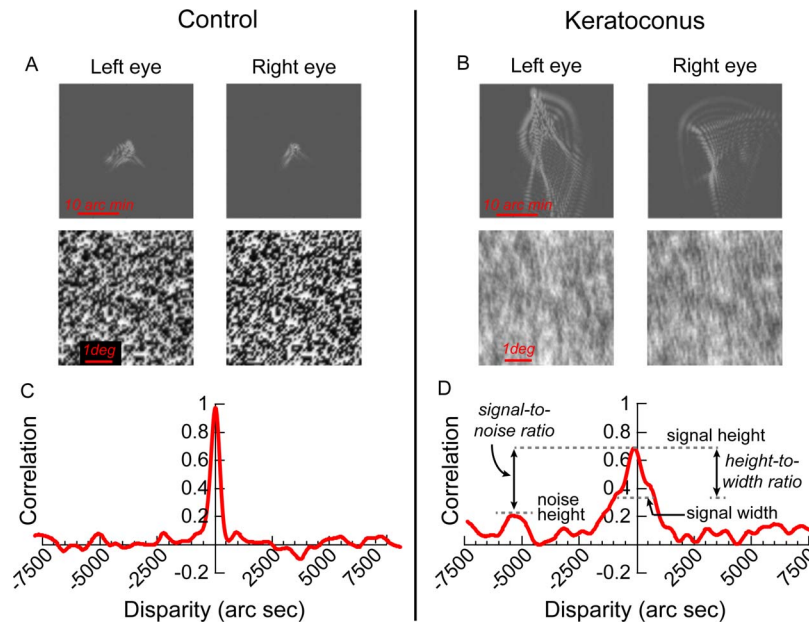


Figure 1. Point-spread functions (top row) were derived from the high-order aberrations of the right and left eyes of a healthy subject (A) and one with bilateral keratoconus (B). They were used to convolve a flat random-dot image to create optically filtered image pairs (bottom row, A–B) representing the retinal image limited by the high-order aberrations of the right and left eyes. 1-D (horizontal) cross-correlation functions were obtained from right- and left-eye retinal images of a healthy subject (C) and a subject with keratoconus (D) to assess the disparity noise (peaks away from zero) and the strength (sharpness and height) of the match for the disparity signal (stimulus disparity). Cross-correlation functions derived from random-dot stereograms convolved with native high-order aberrations of subjects with keratoconus (D) had a lowered peak, an increased spread of the signal peak, and increased noise peaks in comparison to healthy subjects. Also of interest is a shift in the signal peak to a nonzero best matched stimulus disparity. Binocular cross-correlation metrics used in the current study are also described in (D).

defocus and astigmatism terms that correspond to the subject's spherocylindrical refractive error assumes that LOAs were corrected during the disparity calculations. This assumption may not be valid empirically, given the difficulties involved in arriving at the endpoint of subject refraction in eyes with keratoconus. Nevertheless, this approach estimates the impact of HOAs on disparity processing without influence of LOAs. The PSF was computed from the HOAs for each eye with a pixel resolution that was matched with the angular subtense of the dots in the RD image. The RD image was convolved separately with the PSFs for the right and left eyes, and a binocular disparity map was computed with the cross-correlation function between the convolved retinal images of the two eyes (Figure 1A, 1B; Banks et al., 2004; Cormack et al., 1991; Doi et al., 2011; Filippini & Banks, 2009). The two-dimensional (2-D) normalized cross correlation of right and left image pairs was implemented in MATLAB using an algorithm that closely followed the formula from Lewis (1995):

$$\gamma(u, v) = \frac{\sum_{x,y} [f(x, y) - \bar{f}_{u,v}] [t(x - u, y - v) - \bar{t}]}{\left\{ \sum_{x,y} [f(x, y) - \bar{f}_{u,v}]^2 \cdot \sum_{x,y} [t(x - u, y - v) - \bar{t}]^2 \right\}^{0.5}}, \quad (1)$$

where  $f$  is the left eye's image,  $\bar{t}$  is the mean of the right eye's image (which is the template for the purposes of the formula), and  $\bar{f}_{u,v}$  is the mean of  $f(x, y)$  in the region under the template.

Large windows were used in the cross correlation to identify global variations of disparity within relatively small regions in the frontoparallel plane. The application of the cross-correlation algorithm yields a resultant matrix of coefficients for congruency of pairs of dots as one eye's image is translated with respect to the other, representing a disparity map of true and false (spurious) binocular matches. One relative position of the two RD images yields the maximum coefficient value and signifies the highest disparity signal (i.e., a stimulus disparity match). The coefficients range in value from  $-1.0$  (perfect anti-correlation) to  $+1.0$  (perfect correlation). A 1-D slice of the resultant function—that is, the horizontal cross-correlation function—is then extracted (Figure 1C, 1D). This would be derived from a constrained transformation of one eye's image with respect to the other along the horizontal axis through the maximum correlation value obtained. The horizontal cross correlation is most relevant to computing the horizontal binocular disparity stimulus map for empirical measures of stereoacuity. In extracting the

function through the maximum correlation value for the disparity map, we built in a relaxation of the epipolar constraint (Howard & Rogers, 2012). In effect, by not confining the movement of the right eye's image to a horizontal line through the midpoint of the left eye's image, we disregarded the introduction of any potential spurious vertical disparities. It is likely that abnormal aberrations will influence the estimate of depth magnitude and surface orientation by degrading vertical disparity or introducing spurious vertical disparities. Vertical disparity is a cue used to estimate distance and azimuth, which are needed to scale depth magnitude from horizontal disparity and surface orientation (i.e., slant about a vertical axis; Backus, Banks, van Ee, & Crowell, 1999; Gillam et al., 1988; Howard & Rogers, 2012; Mayhew & Longuet-Higgins, 1982). We quantify the impact of optical aberrations on horizontal disparity only, due to its prominent relevance in computing stereo thresholds.

### Cross-correlation metrics

Cross-correlation functions of subjects with and without keratoconus were quantified using several metrics (Figure 1C, 1D). The signal width was defined as the full width at half maximum of the cross-correlation signal. It represents the range of disparities over which the correlation coefficient remained above 50% of the maximum value and describes the signal spread or disparity blur induced by the optical degradation. The signal height, defined as the height of the peak positive value of the cross correlation, signifies the best-matched position, estimating the disparity signal strength. The noise height, defined as the height of the peak positive *incorrect* match, represents the magnitude of disparity noise. The signal-to-noise ratio estimates the fidelity of the cross-correlation signal as a ratio of the signal height to the noise height. The height-to-width ratio describes the sharpness or kurtosis of the disparity signal match. It estimates the disparity resolution as a ratio of the signal height to the signal width.

It is assumed that both the disparity signal and the noise were equally affected by optically induced blurring. This includes the loss of retinal image contrast (equal or unequal in the two eyes) and the phase distortion or displacement of corresponding image locations for the two eyes. We predicted that increased disparity noise due to different phase distortions in the two eyes and lowered disparity resolution due to optical differences in contrast between the two eyes could contaminate the computed binocular retinal disparity signal and make the extraction of stereoacuity more difficult.

## Statistical analyses

All empirical and computational data were analyzed using Microsoft Excel and SPSS (Version 25). Group data are presented as ranges of minimum to maximum values for nonnormally distributed data or as mean  $\pm$  standard deviation for normally distributed data, unless otherwise specified. Shapiro–Wilk tests were performed to assess normality of the distributions of data prior to the drawing of statistical inferences from correlations of data. When the data were approximately normally distributed, were linear, and had no significant outliers, Pearson's correlations were performed. When any one variable being compared failed these assumptions, Spearman's rank order correlations were performed to assess any apparent monotonic relationships in the scatterplots. The data obtained from subjects with keratoconus in the HOA uncorrected and HOA minimized conditions were sometimes combined with the data from control subjects to obtain a continuum of data from high to low magnitudes of HOAs. This combined data set was then used to examine the relationships between computationally derived data and empirical stereoacuity. Instances where data were combined or individually analyzed are stated explicitly in the results.

Distributions of the cross-correlation metrics derived from the native PSFs and the two manipulations that rendered the same PSFs mirror symmetric and rotationally symmetric were compared using a nonparametric Friedman test. Post hoc analyses with Wilcoxon signed-rank tests with Bonferroni corrections applied were used to compare pairs of these conditions when significant. Also, the effects of the native contrast (modulation transfer function [MTF]) on the cross-correlation metrics when the phase transfer function (PTF) was nulled were compared between the subjects with and without keratoconus subjects using a Mann–Whitney U test.

## Specific methods and results

The interested reader is directed to the Appendix for the ranges of high-order root mean square (HORMS), visual acuity, and stereoacuity for the subjects in the study. Also included in the Appendix is a Zernike-component model, which simulates the PSFs of individual or simple combinations of Zernike aberrations for each eye and illustrates the effects of certain interocular combinations of Zernike aberrations on the cross-correlation metrics.

We present the specific methods and results to address each of the three goals of the study in tandem arrangement in separate sections.

Variables correlated with empirical stereoacuity thresholds	Spearman's rho ( $r_s$ )	$p$
Cross-correlation signal width <sup>#</sup>	0.65	<0.001***
Cross-correlation signal height	−0.79	<0.001***
Cross-correlation signal-to-noise ratio	−0.85	<0.001***
Cross-correlation signal height-to-width ratio <sup>#</sup>	−0.75	<0.001***
Interocular VSOTF averages	0.34	0.07
Interocular VSMTF averages	−0.42	<0.05*
Interocular differences in VSOTF	−0.03	0.9
Interocular differences in VSMTF	0.09	0.7
Interocular VSOTF ratios	0.45	<0.05*
Interocular VSMTF ratios	0.41	<0.05*

Table 1. Spearman's correlations for combined data variables computed from native aberration data scaled to 6-mm pupils were compared with empirical stereoacuity thresholds that were also obtained at 6 mm ( $n = 29$ ). Notes: <sup>#</sup> $n = 25$ . \* $p < 0.05$ ; \*\*\* $p < 0.001$ .

### Relationships between binocular cross-correlation metrics and stereoacuity

The goal of the analysis was to determine the effects of HOAs on cross-correlation metrics that pertain to disparity visibility—that is, contrast and phase distortions of the two eyes' retinal images—and their potential effect on binocular matching for retinal disparity and stereoacuity thresholds.

#### Methods

Binocular cross-correlation metrics were computed using aberrations from subjects with keratoconus with

HOAs uncorrected and with HOAs minimized by RGP CL wear and from control subjects with their spectacle refractive corrections. The metrics were then correlated with corresponding empirical measures of stereoacuity to make inferences about the contribution of HOAs to stereoacuity in subjects with and without keratoconus. Interocular differences in phase distortions and contrast due to HOAs would both be expected to lead to suboptimal binocular cross-correlation metrics.

#### Results

Relationships between data for pupils scaled to 6 mm and stereoacuity thresholds are indicated by the Spearman's rho and the corresponding  $p$  values in Table 1; only the details of the significant monotonic relationships are shown in Figures 2 and 3. The metrics of signal width, signal height, signal-to-noise height ratio, and signal height-to-width ratio obtained from the horizontal cross-correlation functions were all statistically significant for strong to very strong monotonic correlations with stereoacuity.

### IQ metrics estimate the effects on stereoacuity of contrast losses due to HOAs

The covariation of binocular cross-correlation metrics with stereoacuity performance would not inform us about the independent impacts of contrast reductions or phase distortions on stereoacuity, since they would both likely influence the relationship. Therefore, as a first step to explore the impact of visual performance

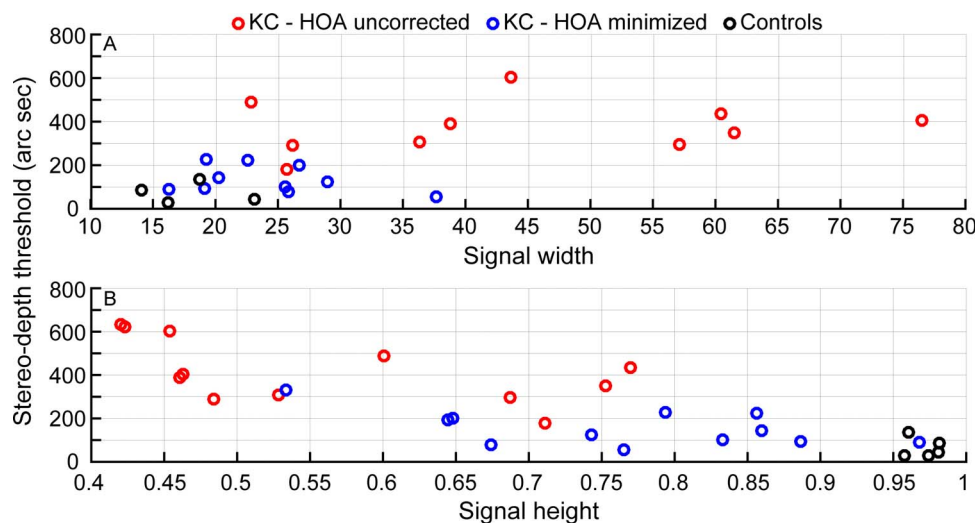


Figure 2. Comparisons of the cross-correlation signal width (top) and signal height (bottom) computed for 6-mm pupils with stereoacuity thresholds. Red circles indicate data for the condition with uncorrected (spectacles) high-order aberrations, and blue circles indicate the data for the condition with high-order aberrations minimized (rigid gas-permeable contact lenses). In the top panel,  $n = 10$ , since signal-width computations were not possible in two instances; in the bottom panel,  $n = 12$ . The black circles denote control data ( $n = 5$ ). Spearman's rho ( $r_s$ ) values were 0.65 (top) and −0.79 (bottom), indicating strong monotonic relationships.

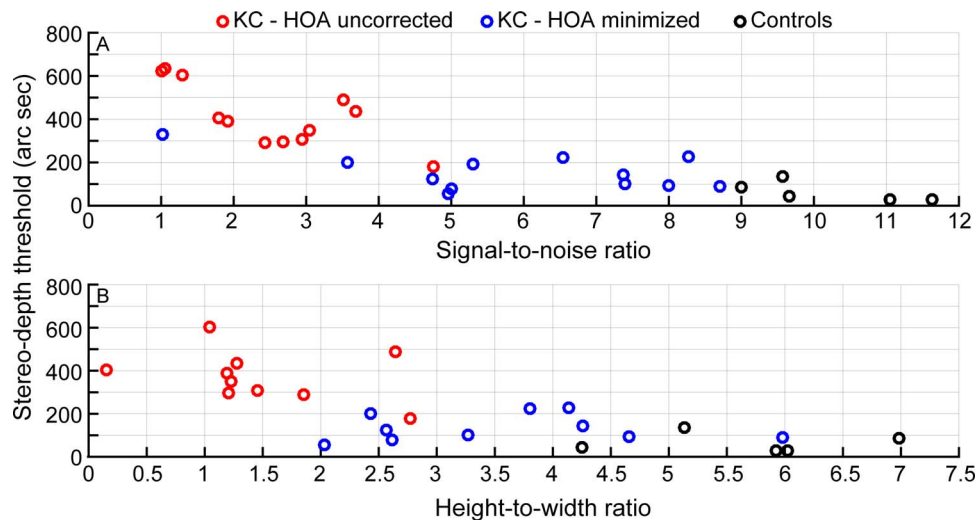


Figure 3. Comparisons of the cross-correlation signal-to-noise ratio (top) and signal height-to-width ratio (scaled up by 100, for convenient visualization; bottom) are compared with stereoacuity thresholds. Red circles indicate data for the condition with uncorrected high-order aberrations (spectacles), and blue circles indicate the data for the condition with high-order aberrations minimized (rigid gas-permeable contact lenses). In the top panel,  $n = 12$ ; in the bottom panel,  $n = 10$ , since signal-width computations were not possible in two instances. The black circles denote control data ( $n = 5$ ). Spearman's rho ( $r_s$ ) values were  $-0.85$  (top) and  $-0.75$  (bottom), indicating very strong and strong monotonic relationships.

based on contrast alone, we computed IQ metrics and explored interocular relationships of IQ metrics against stereoacuity. IQ metrics are scalars used to describe the retinal image quality of grating patterns (Thibos, Hong, Bradley, & Applegate, 2004).

### Methods

IQ metrics that estimate the potential visual performance of each eye limited by contrast loss allowed us to explore how contrast influenced computation of binocular disparity. We chose two IQ metrics that factor in the human eye's neural contrast sensitivity function for further investigation. The VSOTF (visual Strehl ratio computed in the frequency domain [OTF method]) predicts visual performance and is correlated with commonly used empirical measures like visual acuity (Cheng, Bradley, & Thibos, 2004; Marsack, Thibos, & Applegate, 2004; Thibos et al., 2004). The VSMTF (visual Strehl ratio computed in the frequency domain [MTF method]) describes the variation in contrast and, by design, the effects of a well-centered PSF without the effects of phase shifts (Thibos et al., 2004). VSOTF and VSMTF were computed from optical data gathered in subjects with keratoconus with HOAs uncorrected (i.e., unaided or spectacle-corrected condition) and with HOAs minimized by wearing RGP CLs and in control subjects. Since these scalars are estimates of monocular visual performance, we computed interocular averages, absolute interocular differences, and interocular ratios (better/worse eye) and explored how interocular relationships for each of these

IQ metrics covaried with empirical stereo-threshold estimates for the respective conditions.

### Results

Interocular VSMTF averages and interocular ratios of both VSOTF and VSMTF for pupils scaled to 6 mm showed moderate monotonic correlations with stereoacuity (data shown in Table 1; only significant data shown in Figure 4). In particular, without the effects of phase shifts, the relationship between stereo threshold and the VSMTF metric is dominated by contrast losses due to HOAs (Figure 4). The independent effects from phase shifts or contrast losses due to HOAs are more difficult to interpret in this manner since it is unclear which of these interocular relationships has the greatest impact on the cross-correlation function and which predominate in individual subjects.

### Independent contributions of the phase and contrast components of the OTF on cross-correlation metrics

We wanted to computationally analyze the distinct effects of phase and amplitude (contrast) components of the Fourier transform of the PSF (i.e., the OTF) on the cross-correlation metrics and in turn understand their relationship to disparity processing and stereoacuity loss in keratoconus.

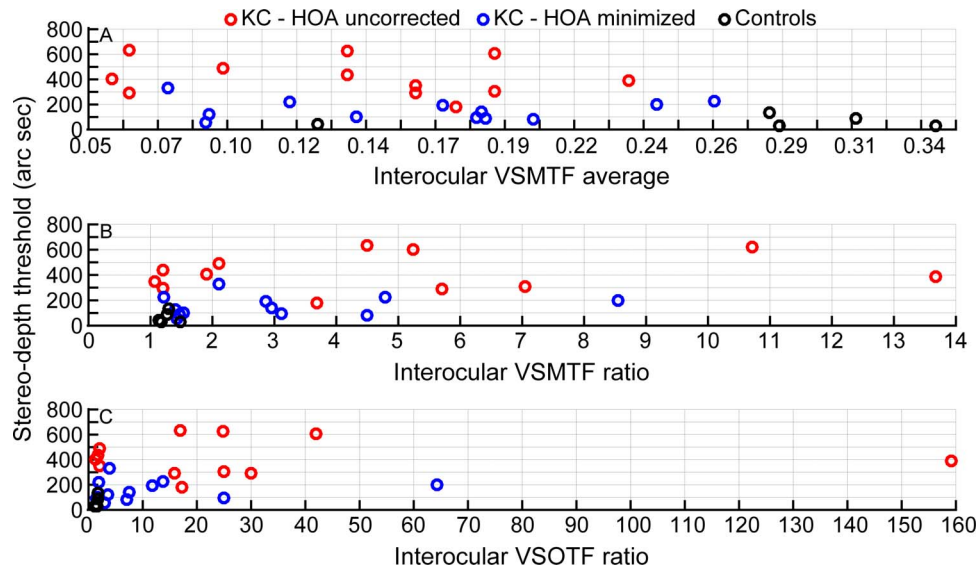


Figure 4. Comparisons of image-quality metrics—interocular averages of VSMTF (top) and interocular VSOTF (middle) and VSMTF (bottom) ratios—computed for 6-mm pupils, with stereoacuity thresholds. Red circles indicate data for the condition with high-order aberrations uncorrected (spectacles;  $n = 12$ ), and blue circles indicate the data for the condition with high-order aberrations minimized (rigid gas-permeable contact lenses;  $n = 12$ ). The black circles denote control data ( $n = 5$ ). Spearman's rho ( $r_s$ ) values were  $-0.42$  (top),  $0.45$  (middle), and  $0.41$  (bottom), indicating moderate monotonic relationships.

## Methods

*Effects of phase:* Might phase distortions, introduced by aberrations like coma that are not rotationally symmetric and seen in large magnitudes in keratoconus, cause significant problems with disparity sensitivity and interfere with stereoacuity? The distinct contribution of the OTF's phase component was estimated by the following process:

- i. Setting the PTF to zero. The new PSF generated following this computational manipulation of the OTF would demonstrate any influence of the phase component of the OTF. Given that the phase component governs the final shape of the PSF, this manipulation centers the new PSF and causes it to be mirror symmetric (note: *not* rotationally symmetric) without the effects of phase shifts (Figure 5B). Improvements in cross-correlation metrics following removal of phase distortions in this manner provide an estimate of their influence on disparity processing.
- ii. Setting the PTF to zero in addition to rendering the MTF rotationally symmetric. This renders the new PSFs rotationally symmetric, making the distribution of contrast symmetric across all orientations while keeping the same overall contrast that was originally available to the eyes. In effect, this centers the new PSFs and makes their shape the same across eyes and conditions, while allowing contrast to vary across eyes (keeping the original overall contrast for a given eye; Figure 5C).

Cross-correlation analysis was repeated for 6-mm pupils using the newly generated PSFs following these zero-phase manipulations (Figure 5B, 5C), and the metrics obtained were compared with those obtained for native PSFs (Figure 5A). The independent effects of phase on cross correlation (and therefore disparity computations) were investigated through metrics quantifying select features of the cross-correlation function—that is, signal width, signal height, and signal-to-noise and signal height-to-width ratios—for individual subjects (for 6-mm pupils).

*Effects of contrast:* The cross-correlation metrics obtained after setting the PTF to zero also enable us to evaluate the effects of contrast alone, independent of the effects of phase. The metrics obtained from both steps just explained, where  $PTF = 0$ , were compared between subjects with keratoconus (combining data for uncorrected and minimized HOAs) and without. We anticipated that the increased HOAs would cause contrast anomalies in keratoconus, while the HOA-induced contrast losses would be within normal limits in healthy subjects.

## Results

*Effects of phase:* The data are shown in Figures 6–9. Data for individual subjects with keratoconus corrected with spectacles (HOA uncorrected, left panel) and with RGP CLs (HOA minimized, middle panel), as well as control subjects (Control, right panel), are plotted separately to better elucidate the effects of HOAs.

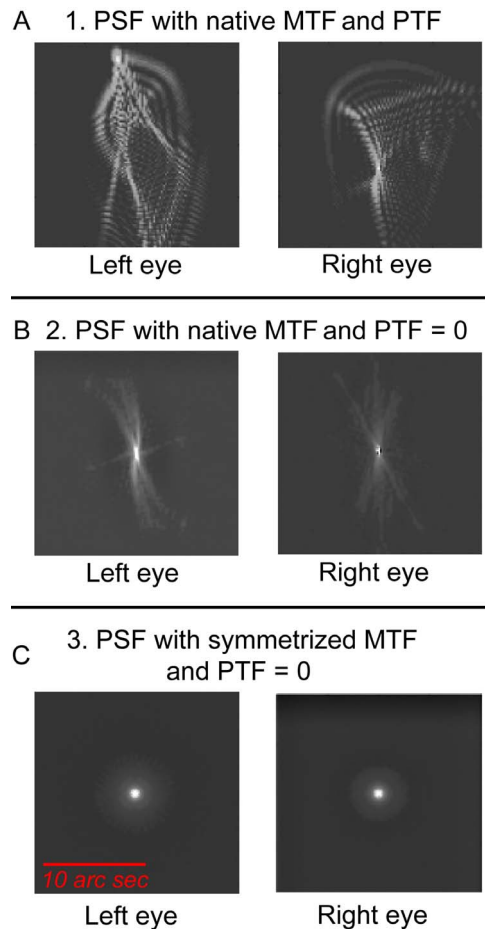


Figure 5. Illustration of optical transfer function manipulation conditions to estimate only the effects of contrast demodulation of the two eyes' images. Point-spread functions (PSFs) for high-order aberrations were derived for three manipulations: (1, top row) native modulation (modulation transfer function) and phase (phase transfer function, PTF), (2, middle row) after setting the PTF to zero to remove phase distortions, and (3, bottom row) after making the modulation transfer function symmetric across all orientations in addition to setting the PTF to zero. Since the phase governs the final shape of the PSF, setting the PTF to zero makes the new PSF mirror symmetric in the middle row, and making the modulation transfer function symmetric makes the new PSF rotationally symmetric in the bottom row. In the third symmetrized condition, the PSF has the same shape across eyes and conditions, while allowing contrast to remain at its original value for individual eyes. Differences in the PSFs between eyes would reflect the influence of contrast.

The distributions of individual data points for native PSFs, PSFs generated after phase correction of the OTF, and rotationally symmetric PSFs were compared separately for data within each of the panels in the figures using a nonparametric ranked test (Friedman). If significant differences in the distributions were revealed, post hoc analyses with Wilcoxon signed-rank

tests with Bonferroni corrections were applied to compare pairs of these conditions.

In general, the OTF phase manipulations had a significant effect on the metrics in the conditions with HOA uncorrected and HOA minimized. There was a reduction in correct-match signal width and an increase in disparity signal height, in addition to a reduction in the nonzero disparity noise. These effects would increase the signal-to-noise and height-to-width ratios compared with data obtained with native PSFs in subjects with keratoconus. Inspection of the figures reveals that there was a tighter spread of all three metrics after the PSF manipulations. More specifically, in subjects with keratoconus and spectacles, where we assume LOAs are fully corrected (HOA uncorrected), Friedman's-test comparisons revealed significant differences between the distributions of all three cross-correlation metrics following PSF manipulations (see results for the left panel in Table 2 and Figures 6–9). When HOAs were minimized in the same subjects with RGP CLs, distributions did not differ significantly for signal width but were significantly different for signal height and signal-to-noise and signal height-to-width ratios (see results for the middle panel in Table 2 and Figures 6–9).

The native PSFs in control subjects (Condition 1 in the right panel of Figures 6–9) were more centered and more symmetric between the two eyes than in subjects with keratoconus, suggesting that control subjects had less phase distortion at the outset. Therefore, similar comparisons of PSF phase manipulations in control subjects showed a diminished benefit of these manipulations, where distributions were different only for signal heights.

Frequently, post hoc paired comparisons showed that both zero-phase manipulations (Conditions 2 and 3) improved the cross-correlation metrics from the native condition (1), suggesting that the native phase is detrimental to estimating binocular disparity. Specifically, for keratoconus there were statistically significant differences seen between PSF conditions in several paired comparisons except for signal width, as mentioned in the captions for Figures 6–9.

*Effects of contrast:* Both computational adjustments of the PSF (Condition 2: MTF<sub>n</sub>, PTF<sub>0</sub>; Condition 3: MTF<sub>sm</sub>, PTF<sub>0</sub>) shown in Figures 6–9 are conditions in which the effects of phase distortions of the OTF have been removed, leaving behind the effects of contrast alone. We compared the keratoconus data for left and middle panels combined in each figure (HOA uncorrected and HOA minimized), with the control data plotted in the right panel to estimate how improving the contrast of the PSF alone in keratoconus might improve the cross-correlation metrics.

The contrast losses due to increased HOAs alone in keratoconus influenced cross-correlation metrics and

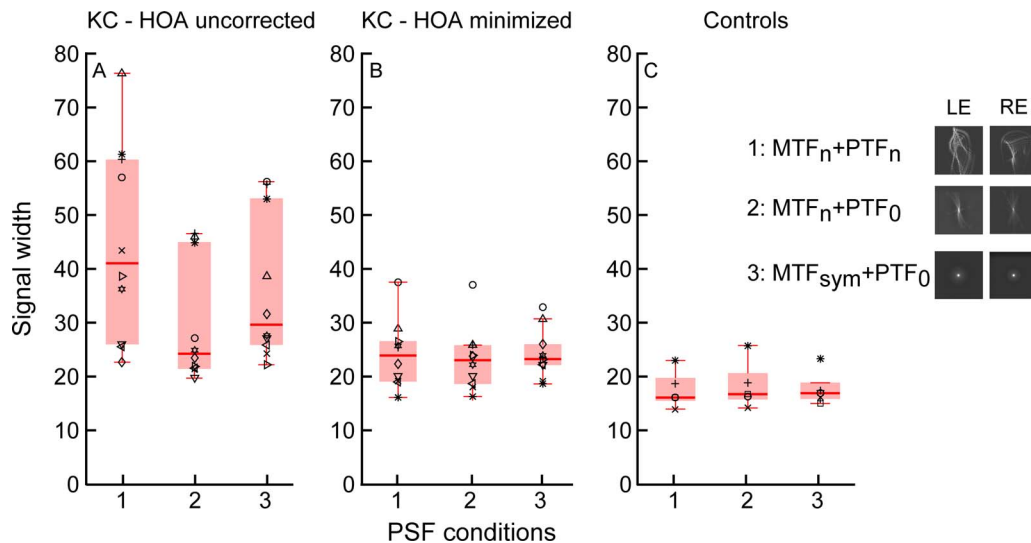


Figure 6. Box-and-whisker plot comparisons of the signal width computed with native point-spread functions (PSFs; 1: MTF<sub>n</sub>, PTF<sub>n</sub>), PSFs generated from phase-corrected optical transfer functions (2: MTF<sub>n</sub>, PTF<sub>0</sub>), and PSFs generated from rotationally symmetric modulation transfer functions (3: MTF<sub>sym</sub>, PTF<sub>0</sub>) over 6-mm pupils. The left panel indicates comparisons for the condition with high-order aberrations uncorrected (estimates the spectacle condition), the middle panel has data from the condition with high-order aberrations minimized (rigid gas-permeable contact lenses) in the same subjects with keratoconus, and the right panel has control data. Individual-subject data are shown in each panel ( $n = 10$  for subjects with keratoconus in the left and middle panels;  $n = 5$  for control subjects in the right panel). The horizontal line within the box indicates the median, and the lower and upper edges of the box indicate the 25th and 75th percentiles. The lower and upper whiskers denote the 1st and 99th quartiles, and data that fall outside the whiskers indicate outliers. A post hoc paired comparison was significant between PSF Conditions 1 and 2 ( $p < 0.01$ ) and 2 and 3 ( $p < 0.05$ ) in the left panel.

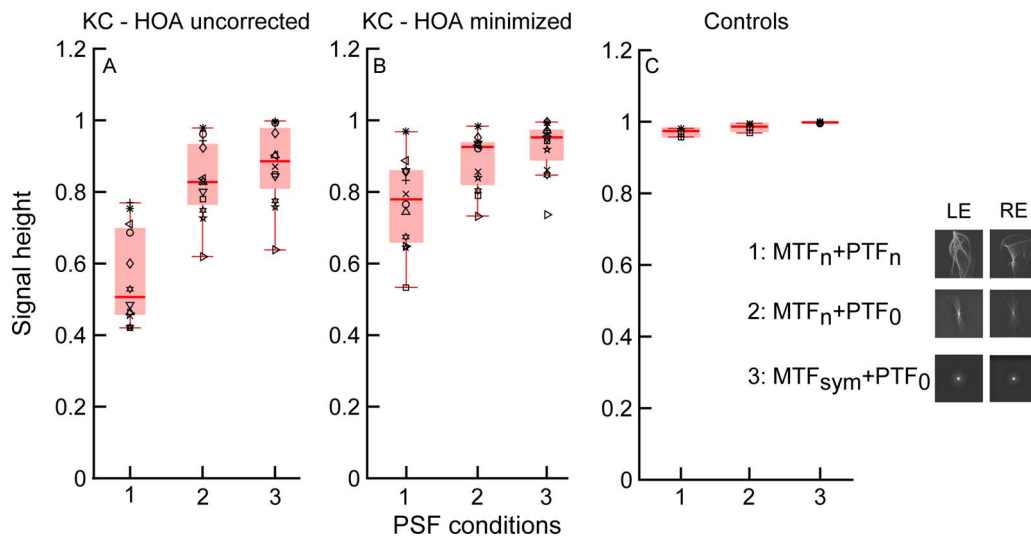


Figure 7. Box-and-whisker plot comparisons of signal heights computed with native point-spread functions (PSFs; 1: MTF<sub>n</sub>, PTF<sub>n</sub>), PSFs generated from phase-corrected optical transfer functions (2: MTF<sub>n</sub>, PTF<sub>0</sub>), and PSFs generated from rotationally symmetric modulation transfer functions (3: MTF<sub>sym</sub>, PTF<sub>0</sub>) over 6-mm pupils. The left panel has data from the condition with high-order aberrations uncorrected (estimates the spectacle condition), the middle panel has data from the condition with high-order aberrations minimized (rigid gas-permeable contact lenses) in the same subjects with keratoconus, and the right panel has control data. Individual-subject data are shown in each panel ( $n = 12$  for subjects with keratoconus in the left and middle panels;  $n = 5$  for control subjects in the right panel). The horizontal line within the box indicates the median, and the lower and upper edges of the box indicate the 25th and 75th percentiles. The lower and upper whiskers denote the 1st and 99th quartiles, and data that fall outside the whiskers indicate outliers. A post hoc paired comparison was significant between all pairs of PSF conditions ( $p < 0.05$ ) in the left and middle panels, and between Conditions 1 and 2 and Conditions 1 and 3 ( $p < 0.01$ ) in the right panel.

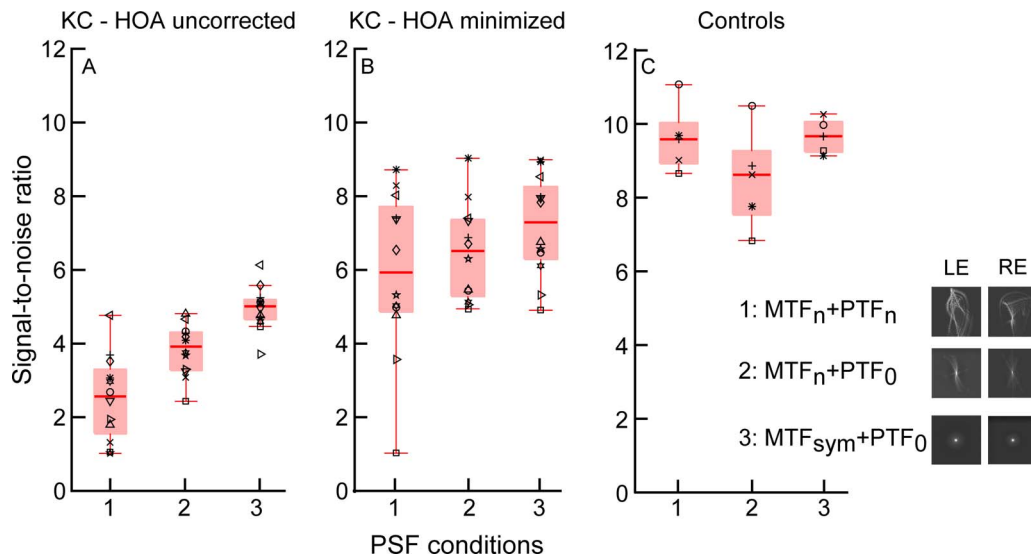


Figure 8. Box-and-whisker plot comparisons of signal-to-noise ratios computed with native point-spread functions (PSFs; 1: MTF<sub>n</sub>, PTF<sub>n</sub>), PSFs generated from phase-corrected optical transfer functions (2: MTF<sub>n</sub>, PTF<sub>0</sub>), and PSFs generated from rotationally symmetric modulation transfer functions (3: MTF<sub>sym</sub>, PTF<sub>0</sub>) over 6-mm pupils. The left panel has data from the condition with high-order aberrations uncorrected (estimates the spectacle condition), the middle panel has data from the condition with high-order aberrations minimized (rigid gas-permeable contact lenses) in the same subjects with keratoconus, and the right panel has control data. Individual-subject data are shown in each panel ( $n = 12$  for subjects with keratoconus in the left and middle panels;  $n = 5$  for control subjects in the right panel). The horizontal line within the box indicates the median, and the lower and upper edges of the box indicate the 25th and 75th percentiles. The lower and upper whiskers denote the 1st and 99th quartiles, and data that fall outside the whiskers indicate outliers. A post hoc paired comparison was significant between all pairs of PSF conditions ( $p < 0.01$ ) in the left panel, and between Conditions 1 and 3 and Conditions 2 and 3 ( $p < 0.01$ ) in the middle panel.

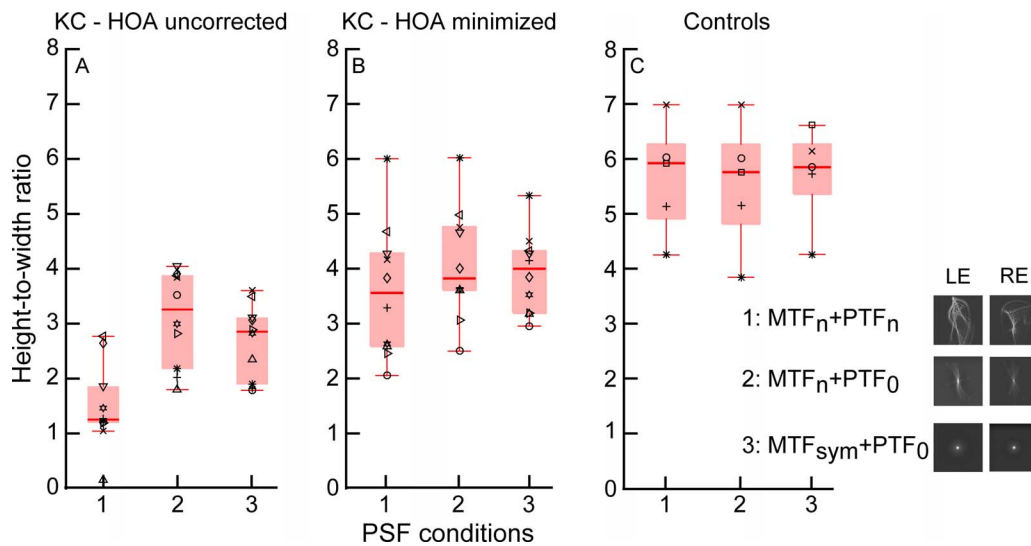


Figure 9. Box-and-whisker plot comparisons of height-to-width ratios computed with native point-spread functions (PSFs; 1: MTF<sub>n</sub>, PTF<sub>n</sub>), PSFs generated from phase-corrected optical transfer functions (2: MTF<sub>n</sub>, PTF<sub>0</sub>), and PSFs generated from rotationally symmetric modulation transfer functions (3: MTF<sub>sym</sub>, PTF<sub>0</sub>) over 6-mm pupils. The left panel indicates comparisons in the condition with high-order aberrations uncorrected (estimates the spectacle condition), the middle panel has data from the condition with high-order aberrations minimized (rigid gas-permeable contact lenses) in the same subjects with keratoconus, and the right panel is control data. Individual-subject data are shown in each panel ( $n = 10$  for subjects with keratoconus in the left and middle panels;  $n = 5$  for control subjects in the right panel). The horizontal line within the box indicates the median, and the lower and upper edges of the box indicate the 25th and 75th percentiles. The lower and upper whiskers denote the 1st and 99th quartiles, and data that fall outside the whiskers indicate outliers. A post hoc paired comparison was significant between all pairs of PSF conditions ( $p < 0.05$ ) in the left panel, and between Conditions 1 and 2 ( $p < 0.01$ ) in the middle panel.

	HOA uncorrected, left panel			HOA minimized, middle panel			Control, right panel		
Friedman's-test comparison results	<i>n</i>	$\chi^2(2)$	<i>p</i>	<i>n</i>	$\chi^2(2)$	<i>p</i>	<i>n</i>	$\chi^2(2)$	<i>p</i>
Signal width (Figure 6)	10	10.4	0.01	10	2.6	0.27	5	3.6	0.17
Signal height (Figure 7)	12	24.0	<0.001	12	23.5	<0.001	5	9.3	<0.01
Signal-to-noise ratios (Figure 8)	12	20.2	<0.001	12	14.0	<0.001	5	4.8	0.09
Height-to-width ratios (Figure 9)	10	16.8	<0.001	10	9.8	<0.01	5	1.3	0.53

Table 2. Distributions of the cross-correlation metrics derived from (1) native point-spread functions and the two manipulations that rendered the same PSFs (2) mirror symmetric and (3) rotationally symmetric were compared using a nonparametric Friedman test. The tabulated test results show the sample size (*n*),  $\chi^2(2)$ , and statistical significance (*p*) values for comparisons between the three point-spread-function conditions for each of the metrics and conditions of high-order aberrations (HOAs) listed.

negatively affected estimates of binocular disparity. We conclude this from examining contrast for Condition 2 (PTF = 0) in Figures 6–9—where overall, subjects with keratoconus had poorer outcomes than control subjects. The Mann–Whitney *U* test revealed higher mean ranks for the cross-correlation signal width ( $U = 17.0$ ,  $p < 0.05$ ) and lower mean ranks for signal height ( $U = 3.0$ ,  $p < 0.001$ ) and signal-to-noise ( $U = 9.0$ ,  $p < 0.01$ ) and height-to-width ratios ( $U = 10.5$ ,  $p < 0.01$ ). Comparisons between subjects with and without keratoconus for Condition 3, where phase distortions were removed in addition to symmetrizing the distribution of contrast in the PSF, yielded similar results. Specifically, the Mann–Whitney *U* test revealed higher mean ranks for the cross-correlation signal width ( $U = 6.0$ ,  $p < 0.01$ ) and lower mean ranks for signal height ( $U = 10$ ,  $p < 0.01$ ) and signal-to-noise ( $U = 0$ ,  $p = 0.001$ ) and height-to-width ratios ( $U = 3$ ,  $p = 0.001$ ), demonstrating an effect of contrast on cross-correlation parameters that would impair stereopsis.

## Discussion

Subjects with keratoconus may experience significant stereoacuity detriment due to HOAs. Stereo-depth performance of subjects with keratoconus is poorer with spectacle correction (HOA uncorrected) compared to habitual RGP CL correction that corrects LOAs and minimizes HOAs (HOA minimized). Stereoacuity is also impaired in keratoconus by the residual HOAs with RGP CLs, compared to healthy subjects with typical HOAs (Maeda et al., 2002; Marsack, Parker, Pesudovs, Donnelly, & Applegate, 2007; Negishi, Kumanomido, Utsumi, & Tsubota, 2007; Nilagiri et al., 2018). Our goal was to model how aberrations, particularly HOAs, might contribute to the stereoacuity detriment seen with different optical corrections for keratoconus.

Stereoacuity requires matching the image in one eye with the appropriate image in the other eye, widely known as the “stereo correspondence problem” (Banks, Gepshtein, & Rose, 2005; Howard & Rogers, 2012).

This problem is more evident in the case of RD stereograms, but simplified in the modeling exercise by use of identical elements over one plane. The cross-correlation algorithm models the binocular matching process describing the coding of binocular disparity from which stereo depth is extracted. We describe specific cross-correlation metrics and demonstrate their use with simulated aberrations described by Zernike coefficients. We also examine relationships between cross-correlation metrics, derived from empirical HOA measures of subjects with and without keratoconus, and stereoacuity. We then examine the separate effects of phase distortions and contrast loss on binocular cross-correlation metrics and therefore the computation of disparity.

## The influence of the shape of the PSF described by Zernike coefficients on the computation of binocular disparity and interpretation of metrics

The cross-correlation metrics are influenced by the aberrations of each eye and their interocular asymmetries. The width of the peak match or signal width is mainly influenced by the extent of horizontal blur of the two retinal images. If blur of the two ocular images is equal in all respects, then the signal height is 1.0 at zero disparity alignment, but the signal width increases due to partial overlap of images at nonzero alignments of the two ocular images. The signal height would also be influenced by differences in phase distortions of the two ocular images. Phase differences introduce nonzero horizontal disparities when the images are aligned in the fixation plane. These nonzero disparities manifest as noise peaks in the cross-correlation function away from zero disparity alignment. Disparity noise reduces the number of retinal pattern elements aligned with the stimulus disparity and lowers the signal height at zero disparity alignment. Thus, unequal phase distortions in the two eyes will reduce signal height and increase the amplitude of noise peaks away from zero disparity and cause a reduction of the signal-to-noise ratio. Finally, even perfectly matched retinal images of RD stereo-

grams exhibit spurious or false matches, which do not influence signal height when aligned in zero disparity but do introduce spurious or false matches at nonzero disparities, which will also cause slight reductions of the signal-to-noise ratio. Computing cross-correlation metrics with multiple RD patterns would negate the influence of such spurious matches, and was not performed since it was beyond the scope of this article. We found that the signal-height metric is highly correlated with the noise-height metric (Spearman's  $\rho_s = -0.84$ ,  $p < 0.001$ ), suggesting that nonzero disparities are mainly the result of real disparities introduced by phase distortions rather than spurious false matches.

A simple Zernike-component model was created with controlled magnitudes of chosen aberrations and interocular differences of aberrations (see Appendix, Table A1). This provided us with important insights regarding the impact of LOAs in general, and HOAs usually seen in keratoconus, on computation of binocular disparity. The modeling exercise shows the effects that aberrations described by specific Zernike terms have on binocular cross-correlation metrics, which are related to binocular disparity and stereoacuity in healthy and keratoconic eyes. The orientation, shape, and magnitude of the blur produced by aberrations uniquely affect the cross-correlation metrics, as do interocular differences in these PSF characteristics between the two eyes. Note that the RD stimulus characteristics have an effect on the results (White, 1962), and we indeed found that the optimal values of the metrics are different for the vertically and horizontally mirrored RD pattern used in the Zernike-component model (simulation data not shown) compared to the nonmirrored RD pattern that was used for empirical testing of stereopsis in our subjects and in other computational analyses using wavefront data from our subjects.

The current study emphasizes the effect of abnormally large HOAs found in keratoconus on cross-correlation metrics and stereoacuity; and for comparison, we include an analysis of LOAs in the model and our discussion. Comparing the cross-correlation metrics from the Zernike-component model (see Appendix, Table A1) with the empirical stereoacuity results for comparable interocular LOA blur differences investigated by Lovasik and Szymkiw (1985) and Chen et al. (2005), we deduce that both increased signal width (i.e., disparity blur) and lowered signal height-to-width ratios may be associated with suboptimal stereo-task performance. LOAs (Table A1, rows 2–9), even in small amounts, would have an impact, and their significant effects on stereoacuity are evident from our model and these previous studies. Among HOAs, we focused on vertical coma (Table A1, rows 10 and 11) due to its importance in keratoconus (Maeda et al.,

2002; Negishi et al., 2007; Pantanelli, MacRae, Jeong, & Yoon, 2007). Cross-correlation metrics are in the presence of mismatched vertical coma in two eyes that otherwise have equal amounts of defocus, spherical aberration, and astigmatism. Large amounts of the coma that is not rotationally symmetric or mismatches in the magnitudes alone, especially with dilated pupils in these typically young individuals, could pose a problem for stereopsis.

## The influence of HOAs on the strength of binocular retinal disparity signals

Since our subjects wore optical corrections for their LOAs during empirical measures of stereoacuity, we assume perfect correction of LOAs. While this is impractical, we made this assumption so we could make inferences about the influence of HOAs. Based on this assumption, the variation seen in the empirical stereoacuity data would then partly be from HOAs and partly from possible individual neural adaptations to aberrations (not discussed here; Sabesan & Yoon, 2010). HOA magnitudes in our subjects were along a continuum from high to low—that is, higher in subjects with spectacle-corrected keratoconus, followed by the same subjects with RGP CL corrections, and lowest in control subjects (see Appendix, Table A2). The strong covariation of stereoacuity with HORMS averages or HORMS differences between the two eyes (see Appendix, Figure A1, Table A1) suggests that the absolute values of high-order Zernike coefficients in the two eyes are important bases of stereoacuity performance.

By themselves, HORMS relationships between eyes do not give us any information about the relationships between convolved image pairs derived from these eyes, or unique retinal image qualities of our subjects' individual eyes described by their PSFs. The binocular cross-correlation metrics of signal width, signal height, and signal-to-noise and height-to-width ratios, and the IQ metrics VSOTF and VSMTF, may all be valuable in providing this information. Binocular cross-correlation metrics were all uniquely affected by the binocular optical makeup of our subjects' eyes. Overall, the distribution of the four cross-correlation metrics (signal width, signal height, signal-to-noise ratio, and height-to-width ratio) had strong to very strong monotonic relationships with empirical measures of stereoacuity (Table 1, Figures 2–3), suggesting that irregularities of contrast distribution and phase relationships created by HOAs between the two eyes closely corresponded with stereo performance. Additionally, interocular ratios of the two IQ metrics VSOTF and VSMTF, which have been reported to predict visual performance (Cheng et al., 2004; Marsack et al., 2004), showed moderate relationships with stereoacuity (Table 1, Figure 4) as

limited by the contrast loss produced by HOAs. Note that IQ metrics computed with HOAs alone are not representative of the retinal IQ of our subjects, since any small residual LOAs in combination with HOAs may either reduce or improve IQ in these subjects (Applegate, Marsack, Ramos, & Sarver, 2003).

## The contributions of contrast losses and phase shifts to reduced stereoacuity sensitivity

### Contrast losses

While we hypothesized that contrast losses and phase distortions due to HOAs would affect the binocular disparity coding process described by cross correlation, how did these two individual factors influence the cross-correlation results? Stereoacuity is negatively affected by differences in contrast between the two eyes and affected by the contrast paradox (Cormack et al., 1997; Halpern & Blake, 1988; Legge & Gu, 1989; Schor & Heckmann, 1989). Interocular differences in optical blur from HOAs, which would lower contrast at high spatial frequencies in keratoconus, might have similar effects on stereoacuity. Note that in the context of interocular contrast dissimilarities, our algorithm returns a perfect cross-correlation peak of 1 when the RD pattern is correlated with another of the same structure but equally lowered contrast for all dots and spatial frequencies (data not shown). However, in a complex optical anomaly like keratoconus, we would not expect predictable interocular differences in global contrast reductions at all spatial frequencies for corresponding dots. Rather, there could be differential contrast reductions at high versus low spatial frequencies, irregular changes in contrast in the corresponding patches of the two images, or phase shifts and smearing in unequal directions between the two eyes. Indeed, contrast losses from HOAs, uncontaminated by phase, influenced the cross-correlation metrics. This is evident from data comparing keratoconus and controls following phase correction of the OTFs.

### Phase distortions

We predicted that phase distortions would have important effects on the horizontal cross-correlation function; however, not much is known about phase distortions caused by aberrations in relation to stereoacuity. Unequal phase distortions of the two ocular images would reduce signal height, increase the magnitude of nonzero disparities (noise height), and decrease the signal-to-noise ratio.

Figures 6–9 illustrate that setting the phase of the OTF to zero increased the peak signal height in the cross-correlation function, suggesting that phase dis-

tortions might have an impact on stereoacuity performance. However, we must consider that there are interactions between phase and contrast of Fourier components of the PSF. The shape of the PSF is largely governed by the PTF. Phase distortions from HOAs alter the phase relationship between Fourier components of the PSF and its convolution with the stimulus pattern, and this changes the composite contrast of the retinal image (e.g., composite contrast changes when first and third harmonic frequencies in peaks-add phase are changed to peaks-subtract phase with a 180° phase shift of one of the frequencies). Thus, when the phase of the PSF was changed to zero in our simulations, the composite contrast of the PSF and the contrast of its convolution with the RD stereogram were also changed. Given this phase/contrast interaction, our simulations of corrected phase distortions are influenced by composite contrast and are therefore only an approximation of the contribution of phase distortions to image quality. Our simulations are meant to explore the importance of phase versus contrast in governing stereoacuity, but they are for an arbitrary zero-phase relationship for HOAs. Although arbitrary, we believe this analysis has allowed us to glean the relative importance of phase. It has helped establish that HOA-induced phase shifts cause cross-correlation metrics to be suboptimal, and this would potentially hinder stereo performance. Separately, this manipulation provided another means of corroborating that contrast anomalies due to significant magnitudes of HOAs seen in this population would be problematic for stereoacuity, as discussed earlier.

## Predictions of stereo sensitivity from optical aberrations

We can speculate about the agreement between empirical measures of stereo-depth thresholds and the disparity matches predicted by optical aberrations and their corresponding binocular cross-correlation metrics. The stereo loss could either be greater or less than predictions based on several factors. The nature of optical distortions and the difficulty of obtaining a global depth percept with the use of the RD stereogram test on an untrained subject would have an impact on the predictions (Westheimer, 2013; Westheimer & McKee, 1980). A practice session and adequate exposure time, as provided for subjects in this study, would help avoid difficulties due to unfamiliarity or complex processing required for the RD test. It is to be noted that optical aberrations may degrade other tests of stereoacuity, such as line stereograms or front-back juxtaposed real objects, differently. Results in the current study were obtained using a routine clinical tool of RD stereograms, and including other tests for

stereopsis would not necessarily reflect or predict performance of depth perception in natural-viewing scenes where many monocular and binocular depth cues are present. Also, the constant degradation of optics in long-term stable keratoconus could produce a mild form of amblyopia that could impair stereoacuity more than predicted by disparity blur (i.e., increased signal width). Alternatively, neural deblurring (Georgeson & Sullivan, 1975) resulting from adaptation to optical blur could compensate for some of the optical degradation, as also seen by Sabesan and Yoon (2010), and improve stereoacuity sensitivity beyond the limits predicted by optical blur. Empirical measures of these attributes could resolve this issue.

Complex neural and subjective factors determine the percept and visual experience of an individual subject and are responsible for the significant variation in psychophysical measurements obtained in research laboratories. Optical wavefront aberrations of the eye are easily accessible objective measurements. They determine retinal image quality and are the bedrock for further neural processing, whether it is visual acuity or stereoacuity. Several metrics have been derived from wavefront aberrations to predict visual acuity and subjective refraction in subjects with and without keratoconus (Marsack et al., 2004; Pesudovs, Parker, Cheng, & Applegate, 2007; Ravikumar, Marsack, Bedell, Shi, & Applegate, 2013; Ravikumar, Sarver, & Applegate, 2012; Thibos et al., 2004). Similarly, relationships between visual acuity and stereoacuity have long been studied (Donzis, Rappazzo, Burde, & Gordon, 1983; Levy & Glick, 1974), and while the presence of qualitative interrelationships is unequivocal, the predictive value of these relationships is elusive (Sitko et al., 2016). Important in this context is evidence that the retinal blur inherent to the optics of a well-focused healthy eye is not detrimental to stereoacuity (Vlaskamp, Yoon, & Banks, 2011), and that typical stereoacuity cannot serve as a predictor of normal visual acuity (Sitko et al., 2016). Binocular metrics derived from wavefront aberrations, as we did in this study, can potentially be developed further and refined for future clinical predictions of stereoacuity.

## Conclusions

HOAs in keratoconus may cause the significant effects seen on stereoacuity due to both the significant contrast losses and phase distortions, with either contrast or phase effects dominating in individual subjects based on their optical profile. It is likely that LOAs might exert their significant effects on stereoacuity predominantly due to contrast losses, and HOAs may exert their effects via both losses in contrast and

phase distortions. Small residual magnitudes of LOAs dominate the effects of optical aberrations on stereoacuity, and they may be more pertinent in the case of residual aberrations following conventional refractive surgery and will be interesting to study in a future investigation.

*Keywords:* stereoacuity, keratoconus, optical aberrations, cross correlation, disparity

## Acknowledgments

We acknowledge support from NEI K12 EY017269 via the Berkeley Clinical Scientist Development Program and NEI K23 EY024691 to SM, SR/CSRI/189/2013 (G) from the Government of India to SRB (which also supported VKN), NEI T35EY007139 to TTY, and NEI R01EY017678 to CMS. Many thanks to Jianliang Tong and Chris Cantor for general and programming advice, and Jennifer Wong for technical assistance. This work has been presented in parts at the 2015 Association for Research in Vision and Ophthalmology conference in Denver, CO, and the 2016 and 2017 Wavefront Congresses (San Francisco and San Jose, CA, respectively).

Commercial relationships: none.

Corresponding author: Sangeetha Metlapally.

Email: metlapallys@neco.edu.

Address: School of Optometry, UC Berkeley, Berkeley, CA, USA.

## References

- Applegate, R. A., Marsack, J. D., Ramos, R., & Sarver, E. J. (2003). Interaction between aberrations to improve or reduce visual performance. *Journal of Cataract and Refractive Surgery*, 29(8), 1487–1495.
- Backus, B. T., Banks, M. S., van Ee, R., & Crowell, J. A. (1999). Horizontal and vertical disparity, eye position, and stereoscopic slant perception. *Vision Research*, 39(6), 1143–1170.
- Bandela, P. K., Satgunam, P., Garg, P., & Bharadwaj, S. R. (2016). Corneal transplantation in disease affecting only one eye: Does it make a difference to habitual binocular viewing? *PLoS One*, 11(3), e0150118.
- Banks, M. S., Gepshtein, S., & Landy, M. S. (2004). Why is spatial stereoresolution so low? *The Journal of Neuroscience*, 24(9), 2077–2089.
- Banks, M. S., Gepshtein, S., & Rose, H. F. (2005,

- January 16–20). *Local cross-correlation model of stereo correspondence*. Paper presented at the meeting of the International Society for Optics and Photonics (SPIE), San Jose, CA.
- Brainard, D. H. (1997). The Psychophysics Toolbox. *Spatial Vision, 10*(4), 433–436.
- Castro, J. J., Jimenez, J. R., Hita, E., & Ortiz, C. (2009). Influence of interocular differences in the Strehl ratio on binocular summation. *Ophthalmic and Physiological Optics, 29*(3), 370–374.
- Chen, S. I., Hove, M., McCloskey, C. L., & Kaye, S. B. (2005). The effect of monocularly and binocularly induced astigmatic blur on depth discrimination is orientation dependent. *Optometry and Vision Science, 82*(2), 101–113.
- Cheng, X., Bradley, A., & Thibos, L. N. (2004). Predicting subjective judgment of best focus with objective image quality metrics. *Journal of Vision, 4*(4):7, 310–321, <https://doi.org/10.1167/4.4.7>. [PubMed] [Article]
- Cormack, L. K., Stevenson, S. B., & Landers, D. D. (1997). Interactions of spatial frequency and unequal monocular contrasts in stereopsis. *Perception, 26*(9), 1121–1136.
- Cormack, L. K., Stevenson, S. B., & Schor, C. M. (1991). Interocular correlation, luminance contrast and cyclopean processing. *Vision Research, 31*(12), 2195–2207.
- Doi, T., Tanabe, S., & Fujita, I. (2011). Matching and correlation computations in stereoscopic depth perception. *Journal of Vision, 11*(3):1, 1–16, <https://doi.org/10.1167/11.3.1>. [PubMed] [Article]
- Donzis, P. B., Rappazzo, J. A., Burde, R. M., & Gordon, M. (1983). Effect of binocular variations of Snellen's visual acuity on Titmus stereoacuity. *Archives of Ophthalmology, 101*(6), 930–932.
- Duwaer, A. L. (1983). Patent stereopsis with diplopia in random-dot stereograms. *Perception and Psychophysics, 33*(5), 443–454.
- Fielder, A. R., & Moseley, M. J. (1996). Does stereopsis matter in humans? *Eye, 10*(2), 233–238.
- Filippini, H. R., & Banks, M. S. (2009). Limits of stereopsis explained by local cross-correlation. *Journal of Vision, 9*(1):8, 1–18, <https://doi.org/10.1167/9.1.8>. [PubMed] [Article]
- Frost, N. A., Sparrow, J. M., Durant, J. S., Donovan, J. L., Peters, T. J., & Brookes, S. T. (1998). Development of a questionnaire for measurement of vision-related quality of life. *Ophthalmic Epidemiology, 5*(4), 185–210.
- Georgeson, M. A., & Sullivan, G. D. (1975). Contrast constancy: Deblurring in human vision by spatial frequency channels. *Journal of Physiology, 252*(3), 627–656.
- Gillam, B., Chambers, D., & Lawergren, B. (1988). The role of vertical disparity in the scaling of stereoscopic depth perception: An empirical and theoretical study. *Perception and Psychophysics, 44*(5), 473–483.
- Halpern, D. L., & Blake, R. R. (1988). How contrast affects stereoacuity. *Perception, 17*(4), 483–495.
- Harwerth, R. S., & Rawlings, S. C. (1977). Viewing time and stereoscopic threshold with random-dot stereograms. *American Journal of Optometry and Physiological Optics, 54*(7), 452–457.
- Hess, R. F., Liu, C. H., & Wang, Y. Z. (2003). Differential binocular input and local stereopsis. *Vision Research, 43*(22), 2303–2313.
- Howard, I. P., & Rogers, B. J. (2012). *Stereoscopic vision* (Vol. 2). New York: Oxford University Press.
- Jimenez, J. R., Castro, J. J., Hita, E., & Anera, R. G. (2008). Upper disparity limit after LASIK. *Journal of the Optical Society of America A: Optics, Image Science, and Vision, 25*(6), 1227–1231.
- Lam, A. K., Chau, A. S., Lam, W. Y., Leung, G. Y., & Man, B. S. (1996). Effect of naturally occurring visual acuity differences between two eyes in stereoacuity. *Ophthalmic and Physiological Optics, 16*(3), 189–195.
- Legge, G. E., & Gu, Y. C. (1989). Stereopsis and contrast. *Vision Research, 29*(8), 989–1004.
- Levy, N. S., & Glick, E. B. (1974). Stereoscopic perception and Snellen visual acuity. *American Journal of Ophthalmology, 78*(4), 722–724.
- Lewis, J. P. (1995, May). *Fast normalized cross-correlation*. Paper presented at the Vision Interface 95 conference, Quebec City, Canada.
- Lovasik, J. V., & Szymkiw, M. (1985). Effects of aniseikonia, anisometropia, accommodation, retinal illuminance, and pupil size on stereopsis. *Investigative Ophthalmology & Visual Science, 26*(5), 741–750.
- Maeda, N., Fujikado, T., Kuroda, T., Mihashi, T., Hirohara, Y., Nishida, K., ... Tano, Y. (2002). Wavefront aberrations measured with Hartmann-Shack sensor in patients with keratoconus. *Ophthalmology, 109*(11), 1996–2003.
- Marsack, J. D., Parker, K. E., Pesudovs, K., Donnelly, W. J., III, & Applegate, R. A. (2007). Uncorrected wavefront error and visual performance during RGP wear in keratoconus. *Optometry and Vision Science, 84*(6), 463–470.
- Marsack, J. D., Thibos, L. N., & Applegate, R. A. (2004). Metrics of optical quality derived from

- wave aberrations predict visual performance. *Journal of Vision*, 4(4):8, 322–328, <https://doi.org/10.1167/4.4.8>. [PubMed] [Article]
- Mayhew, J. E., & Longuet-Higgins, H. C. (1982, June 3). A computational model of binocular depth perception. *Nature*, 297(5865), 376–378.
- Negishi, K., Kumanomido, T., Utsumi, Y., & Tsubota, K. (2007). Effect of higher-order aberrations on visual function in keratoconic eyes with a rigid gas permeable contact lens. *American Journal of Ophthalmology*, 144(6), 924–929.
- Nilagiri, V. K., Metlapally, S., Kalaiselvan, P., Schor, C. M., & Bharadwaj, S. R. (2018). LogMAR and stereoacuity in keratoconus corrected with spectacles and rigid gas-permeable contact lenses. *Optometry and Vision Science*, 95(4), 391–398.
- O'Connor, A. R., Birch, E. E., Anderson, S., Draper, H., & FSOS Research Group. (2010). The functional significance of stereopsis. *Investigative Ophthalmology & Visual Science*, 51(4), 2019–2023.
- Pantanelli, S., MacRae, S., Jeong, T. M., & Yoon, G. (2007). Characterizing the wave aberration in eyes with keratoconus or penetrating keratoplasty using a high-dynamic range wavefront sensor. *Ophthalmology*, 114(11), 2013–2021.
- Pelli, D. G. (1997). The VideoToolbox software for visual psychophysics: Transforming numbers into movies. *Spatial Vision*, 10(4), 437–442.
- Pesudovs, K., Parker, K. E., Cheng, H., & Applegate, R. A. (2007). The precision of wavefront refraction compared to subjective refraction and autorefraction. *Optometry and Vision Science*, 84(5), 387–392.
- Ravikumar, A., Marsack, J. D., Bedell, H. E., Shi, Y., & Applegate, R. A. (2013). Change in visual acuity is well correlated with change in image-quality metrics for both normal and keratoconic wavefront errors. *Journal of Vision*, 13(13):28, 1–16, <https://doi.org/10.1167/13.13.28>. [PubMed] [Article]
- Ravikumar, A., Sarver, E. J., & Applegate, R. A. (2012). Change in visual acuity is highly correlated with change in six image quality metrics independent of wavefront error and/or pupil diameter. *Journal of Vision*, 12(10):11, 1–13, <https://doi.org/10.1167/12.10.11>. [PubMed] [Article]
- Sabesan, R., & Yoon, G. (2010). Neural compensation for long-term asymmetric optical blur to improve visual performance in keratoconic eyes. *Investigative Ophthalmology & Visual Science*, 51(7), 3835–3839.
- Schor, C., & Heckmann, T. (1989). Interocular differences in contrast and spatial frequency: Effects on stereopsis and fusion. *Vision Research*, 29(7), 837–847.
- Sitko, K. R., Peragallo, J. H., Bidot, S., Biousse, V., Newman, N. J., & Bruce, B. B. (2016). Pitfalls in the use of stereoacuity in the diagnosis of nonorganic visual loss. *Ophthalmology*, 123(1), 198–202.
- Thibos, L. N., Hong, X., Bradley, A., & Applegate, R. A. (2004). Accuracy and precision of objective refraction from wavefront aberrations. *Journal of Vision*, 4(4):9, 329–351, <https://doi.org/10.1167/4.4.9>. [PubMed] [Article]
- Thibos, L. N., Hong, X., Bradley, A., & Cheng, X. (2002). Statistical variation of aberration structure and image quality in a normal population of healthy eyes. *Journal of the Optical Society of America A: Optics, Image Science, and Vision*, 19(12), 2329–2348.
- Tyler, C. W. (1978). Binocular cross-correlation in time and space. *Vision Research*, 18(1), 101–105.
- Vlaskamp, B. N., Yoon, G., & Banks, M. S. (2011). Human stereopsis is not limited by the optics of the well-focused eye. *The Journal of Neuroscience*, 31(27), 9814–9818.
- Westheimer, G. (2013). Clinical evaluation of stereopsis. *Vision Research*, 90, 38–42.
- Westheimer, G., & McKee, S. P. (1980). Stereogram design for testing local stereopsis. *Investigative Ophthalmology & Visual Science*, 19(7), 802–809.
- White, B. W. (1962). Stimulus-conditions affecting a recently discovered stereoscopic effect. *American Journal of Psychology*, 75, 411–420.
- Wood, I. C. (1983). Stereopsis with spatially-degraded images. *Ophthalmic and Physiological Optics*, 3(3), 337–340.

## Appendix

### Zernike-component model of the effects of selected optical aberrations on cross-correlation metrics

A Zernike-component model was developed with selected ideal aberrations of known magnitudes, in order to investigate the effects of individual aberrations, as well as interocular similarities or differences in the magnitude of blur or the shape of the point-spread function (PSF) on the cross-correlation metrics. The PSFs for a diffraction-limited system, low-order aberrations (LOAs), coma, and a typical combination of aberrations that are predominantly found in keratoconus were chosen. Simpler shapes of the PSFs such as these would help us understand, predict, and interpret how more complex blur patterns

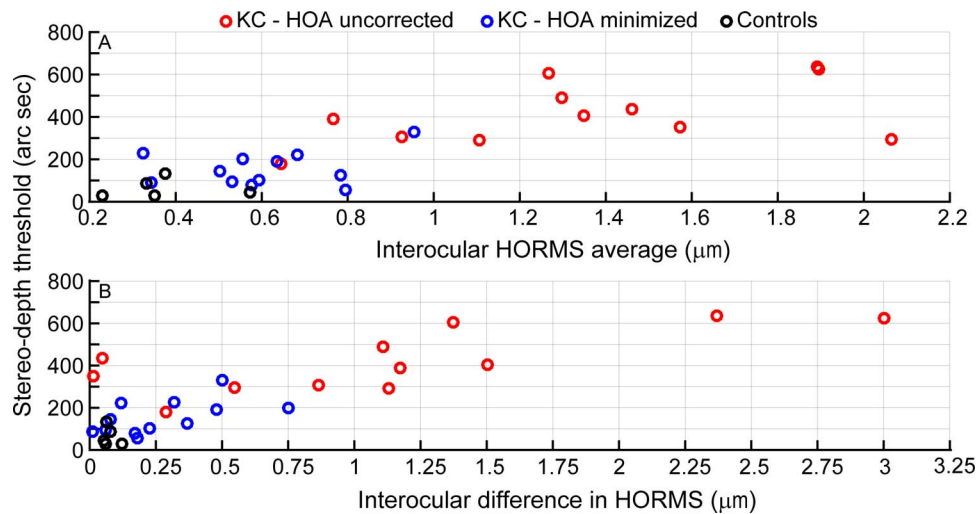


Figure A1. Comparisons of interocular averages (top) and differences (bottom) in high-order root mean square, computed for 6-mm pupils, with stereoacuity thresholds. Red circles indicate the condition with high-order aberrations uncorrected (spectacle), and blue circles indicate the condition with high-order aberrations minimized (rigid gas-permeable contact lenses) for keratoconus ( $n = 12$ ). The black circles denote control data ( $n = 5$ ). Spearman's  $\rho$  ( $r_s$ ) values are 0.78 (top) and 0.65 (bottom), indicating strong monotonic relationships.

or PSFs in keratoconus would influence binocular cross correlation and computations of disparity. For instance, in astigmatism combined with defocus, the smearing of the PSF has a known shape and orientation. Its impact on the binocular cross-correlation metrics could be estimated by simulating astigmatic blur in the same or orthogonal directions for right- and left-eye images. A mirror-symmetric random-dot pattern (i.e., mirroring the upper and lower half and left and right half) was used to avoid any idiosyncratic artifacts introduced by the normally asymmetric random-dot pattern itself.

### Zernike-component-model predictions of the effects of selected aberrations on cross-correlation metrics

Table A1 shows the selected individual Zernike components or combinations of the component aberrations that were modeled to simulate the PSFs of the right and left eyes. As anticipated, the results indicate that two diffraction-limited eyes have close to best outcomes for all the cross-correlation metrics (row 1).

Signal width was greatest in row 7 (worst outcome), with increased horizontal extent of the blur. Symmetric horizontally oriented blur—for example, a positive  $Z_5$  term (described in clinical terminology as *against-the-rule astigmatism*)—spreads the signal more than for vertically oriented blur (row 8). Dots in the random-dot stereogram along the same horizontal latitude are blurred together, causing prominent horizontal streaks. Orthogonal blur differences between the two eyes,

causing differences along the horizontal meridian (rows 3, 9), and increased blur magnitude increase signal width more than the other conditions that we examined. Horizontal blur widens the peak disparity match, which could reduce disparity resolution and stereoacuity. Signal width—that is, disparity blur—is perhaps one of the most important independent metrics.

Signal height is lowered (weakened disparity signal) by any interocular difference in the structure of the PSFs—that is, shape (row 4) and/or magnitude (row 5) or orientation (rows 3, 9) of blur—which could reduce stereoacuity. LOA combinations that were different between the two eyes lowered signal height the most (rows 4, 9). Equal aberrations of the two eyes, even if they are large-magnitude LOA aberrations, result in an ideal signal peak of 1 (rows 2, 6–8).

Disparity noise height is increased (lowering the signal-to-noise ratio) by vertically oriented blur. Dots along the same vertical line of longitude are blurred together, producing prominent nonzero disparity-noise matches. A negative  $Z_5$  term (described in clinical terminology as *with-the-rule astigmatism*; row 8) fares the worst. Disparity noise due to phase distortions would make the stimulus disparity less prominent.

Signal-to-noise ratio is dependent on both the signal height and the noise height, and it is lowered most by unequal defocus between the two eyes (e.g., large anisometropia; row 5), followed by with-the-rule astigmatism in both eyes (row 8), and orthogonally oriented axes of astigmatism in the two eyes (PSF shape differences). A combination of magnitude and shape differences in the blur, as modeled here with pure

Condition (Zernike term manipulated)	PSF right eye	PSF left eye	Signal width	Signal height	Noise height	Signal-to- noise ratio	Height-to- width ratio
1. No aberrations			11.4	1.0	0.13	7.8	8.8
2. Symmetrical astigmatism, Oblique (+ve Z3, +ve Z4)			42.2	1.0	0.18	5.5	2.4
3. Asymmetrical astigmatism, Oblique (+ve Z3, +ve Z4 OD; -ve Z3, +ve Z4 OS)			88.5	0.6	0.21	3.1	0.7
4. Unequal blur (+ve Z4 OD; Z3, +ve Z4 OS)			73.1	0.8	0.21	3.7	1.1
5. Unequal defocus (Nil OD; +ve Z4 OS)			64.8	0.2	0.17	1.3	0.3
6. Equal defocus (+ve value Z4)			60.4	1.0	0.27	3.7	1.7
7. Symmetrical astigmatism, ATR (+ve Z5, +ve Z4)			103.8	1.0	0.22	4.6	1.0
8. Symmetrical astigmatism, WTR (-ve Z5, +ve Z4)			37.3	1.0	0.34	2.9	2.7
9. Asymmetrical astigmatism, ATR- WTR (+ve Z5, +ve Z4 OD; -ve Z5, +ve Z4OS)			79.0	0.6	0.20	3.1	0.8
10. Asymmetrical coma (-ve Z7 OD; Nil OS)			13.3	0.5	0.10	4.8	3.6
11. Asymmetrical coma (typical values of unequal Z7 combined with equal Z4, Z5, Z12)			32.3	0.9	0.25	3.7	2.9

Table A1. Zernike model and simulations of the effects of asymmetries in the shape of the point-spread function (PSF) and magnitude of blur for different low-order aberrations and some high-order aberrations (coma) on the cross-correlation metrics. Z3 = astigmatism (axis 45, 135°); Z4 = defocus; Z5 = astigmatism (axis 90, 180°); Z7 = coma (y-axis or vertical); Z12 = primary spherical aberration.

Group (n)	HORMS range (µm), HOA uncorrected	HORMS range (µm), HOA minimized
Keratoconus, 6-mm pupil (16 eyes)	0.58–3.40	0.16–1.20***
Control, 6-mm pupil (10 eyes)	0.20–0.60	—
Fellow eyes, 6-mm pupil (9 eyes)	0.18–0.75	—

Table A2. Summary of high-order root mean square (HORMS) data over 6-mm pupils in the dataset. Notes: \*\*\* $p < 0.001$  when comparing the HORMS range computed with data from the condition HOA uncorrected (unaided or spectacle corrected) with data from the condition HOA minimized (i.e., corrected by rigid gas-permeable contact lenses) in the same eyes. HOA = high-order aberrations; — = no data for rigid gas-permeable contact lenses; fellow eyes = the contralateral eyes of the dataset for unilateral keratoconus.

defocus in one eye and defocus combined with astigmatism in the other eye (e.g., row 4, “unequal blur”), is also detrimental. Differences in the magnitude of vertical coma between the two eyes, in combination with other LOA terms like defocus, vertical astigmatism, and spherical aberration typically seen in our

Variables correlated with empirical stereoacuity thresholds	Spearman’s rho ( $r_s$ )	$p$
Interocular HORMS averages	0.78	<0.001***
Interocular differences in HORMS	0.65	<0.001***
Interocular HORMS ratios	0.34	0.07

Table A3. Spearman’s correlations for high-order root mean square (HORMS) computed from aberration data scaled to 6-mm pupils, compared with empirical stereoacuity thresholds also obtained at 6-mm ( $n = 29$ ). Notes: \*\*\* $p < 0.001$ .

keratoconus cohort, is detrimental, even if terms other than vertical coma are equal in magnitude between the two eyes.

Signal height-to-width ratio (scaled up by 100, for convenient visualization) is dependent on both the signal height and the signal width, and is lowered by any blur. It is lowered most when there is both an interocular difference and increase in blur, particularly horizontally oriented blur. Unequal defocus and asymmetrical astigmatism reduce this ratio the most (rows 3, 5, 9) and signify reduced sharpness of the peak match.

### **Stereoacuity and magnitude (high-order root mean square) of aberrations in keratoconus**

We present, for the interested reader, the visual acuity, stereoacuity, and high-order root mean square (HORMS) ranges for the subjects included in the study. We also present relationships between stereoacuity data and HORMS, as these are easily available in the clinical setting. LogMAR visual acuity in spectacle-corrected keratoconic eyes through 6-mm apertures ranged from 0.00 to 0.70 (20/20 to 20/100), and in the same group of keratoconic eyes wearing rigid gas-permeable contact lenses, ranged from 0.00 to 0.18 (20/20 to 20/30). Spectacle-corrected LogMAR in fellow eyes of subjects with unilateral keratoconus (8 eyes) and subjects without keratoconus (10 eyes) both ranged from  $-0.12$  to 0.04 (20/15 to 20/22). Empirical stereoacuity thresholds measured with 6-mm apertures in subjects with keratoconus chosen for this study corrected with spectacles ranged from 180 to 635 arcsec, and in the same group of patients wearing rigid gas-permeable contact lenses it ranged from 56 to 330 arcsec. The range of stereoacuity thresholds in the control group was 29–134 arcsec.

HORMS is a standard way of reducing the complex description of the wavefront to one number (in microns) that signifies the optical quality of the eye due to its high-order aberrations. HORMS wavefront error values were calculated for individual eyes for 6-mm

pupils. In order to compare HORMS values with other binocular metrics from the cross correlation or with empirical stereoacuity, they were averaged between the two eyes. Additionally, absolute interocular differences in HORMS and interocular ratios of HORMS (worse/better eye) were computed as potential metrics to describe relationships between the two eyes' optical qualities that might affect estimates of stereoacuity. Data were analyzed separately for eyes without optical correction, eyes corrected by rigid gas-permeable contact lenses, and control eyes.

Table A2 shows a summary of HORMS data, where the data illustrate a significant improvement of HORMS with the reduction of high-order aberrations when keratoconic eyes were corrected with rigid gas-permeable contact lenses. Zernike data for 6-mm pupil diameter were available only in this subset of eyes, due to difficulties encountered with aberrometry measurements in subjects with keratoconus. Wavefront aberration data were also collected in control subjects with high-order aberrations within normal limits, indicated by the relatively low HORMS values over 6-mm pupil diameters. As a separate category, the fellow eyes of subjects with unilateral keratoconus not included in these descriptions had HORMS values that were better than eyes with clinically diagnosed keratoconus, but some had higher HORMS values than the eyes of control subjects.

### **Covariation of HORMS with stereoacuity thresholds**

Relationships between data for pupils scaled to 6 mm and stereoacuity thresholds are indicated by the Spearman's rho and corresponding  $p$  values in Table A1, and only the details of the significant monotonic relationships are shown in Figure A1. Comparisons of both interocular averages and differences in HORMS with stereoacuity thresholds revealed strong positive monotonic relationships.